Submitted to NAMRC 36. Do not cite without written consent of authors.

LASER SURFACE TREATMENT OF A BIODEGRADABLE POLYMER AT VARYING FLUENCES

Anubha Bhatla, Y. Lawrence Yao
Department of Mechanical Engineering
Columbia University
New York, NY 10027

KEYWORDS

Laser, biodegradable, polymer, surface treatment.

ABSTRACT

For biodegradable polymers such as poly (L-lactic acid) (PLLA), material crystallinity has a considerable effect on degradation and physical properties. In this work, the effects of laser fluence of a 355 nm UV Q-switched Nd-YAG laser on the crystallinity and conformation at the surface of PLLA films and the factors affecting the transformation are investigated. Electron microscopy, X-ray diffraction and Infrared spectroscopy are used to study the effects at varying fluences. The melting and crystallization kinetics of PLLA are examined to understand the important parameters that determine the overall crystallinity. Potentially, laser surface treatment at varying fluences can be used to spatially control the generation of a polymer surface with an altered degree of crystallinity. Such a structure may have applications including time released drug delivery.

I. INTRODUCTION

Biodegradable polymers, due to their extensive applications and potential have recently generated significant interest. Poly (α-hydroxy acid) family of polymers, especially poly (lactic acid) (PLA), and its copolymers are particularly important since they are USFDA approved, have desirable properties and degrade, primarily hydrolytically, into bioresorbable products. Their applications include drug delivery devices, fixation plates, tissue engineering, packaging and agriculture. The structure, properties and crystallization of PLA has been reviewed by Garlotta (2001).

In various biomedical applications; it is important to control the surface properties of the polymer especially crystallinity. Tsuji and Ikada (1998) have studied the effect of crystallinity on the degradation of PLA and concluded that hydrolysis of PLA chains initiates in the amorphous regions within and between the spherulites. While other surface treatment methods like coating and plasma treatment can affect surface cell adhesion, structural modifications have not been attempted, as these methods are inherently difficult to control spatially. Although, laser processing of biodegradable polymers has potential due to its flexibility; currently the primary focus has been micro and nano scale fabrication. Laser treatment as a means of surface modification is attractive due to both spatial control and the

ability to control laser properties to control the affected material depth.

Aguilar, et al. (2005) have studied the effects of laser patterning on poly (glycolic acid) (PGA). They observed chemical changes and degradation increase during initial stages of tests in phosphate buffer solution (PBS) without affecting overall degradation time; but did not study the reasons for the affected changes. Lazare and Benet (1993) have used a single excimer pulse to induce periodic roughness on the surface of Mylar (PET) films and with ellipsometric measurements shown formation of thin surface layer with different optical properties but the structural changes were not studied. Dunn and Ouderkirk (1990) have also studied excimer laser texturing of crystalline PET and due to observed increase in refractive index of the treated polymer and IR reflection absorption spectroscopy data suggested that the anisotropy of the surface amorphous layer causes texturing. However, they did not investigate details of the crystal structure changes or factors affecting it.

The main focus of this paper is to utilize laser processing to reduce the crystallinity at the surface of PLA films, to allow for faster surface degradation in the modified regions compared with bulk. Effects of varying fluence on the affected depth are studied. Scanning electron microscopy (SEM), Wide Angle X-ray diffraction (WAXD) and Fourier Transform Infrared spectroscopy (FTIR) are used to analyze the morphology and crystallinity changes at the surface. Factors affecting the laser melting and crystallization of PLA are investigated to study the important parameters and reasons for modified crystallinity post laser irradiation.

II. MELTING AND CRYSTALLIZATION IN POLY (L-LACTIDE)

To consider the effect of laser processing on PLA, it is important to understand the melting and crystallization characteristics of polymers in general and PLA in particular. High Molecular weight PLA is a thermoplastic with a melting temperature of 170-210 ˚C; which being higher than most polymers, makes it suitable for thermal processing. PLA can exist as isomers poly-L-lactide (PLLA) or poly-D-lactide (PDLA); of which PLLA is semicrystalline and can be crystallized by cooling from melt, annealing and under strain. It is known to crystallize by chain folding, forming lamellae perpendicular to the chain axis. While thermodynamics of polymer melting are well studied, the kinetics are still under debate. Polymers show a melting transition over a temperature range, with the equilibrium melting temperature (*Gibbs-Thompson Equation*) varying with the distribution of the lamellar thickness. Nanosecond laser irradiation can cause rapid heating with cooling rates of the order of 10^8 K/s which are much higher than traditional thermal rates of 10-100 K/s. The total amount of the crystallinity in the material is a function of nucleation and growth which are a strong function of the cooling rate. In general, in polymers, melting is a fast process completed with low superheating versus crystallization which is a relatively slower process requiring high supercooling. Crystallization studies of PLLA have shown that the kinetics of melt crystallization of PLLA are relatively slow and hence the possibility of affecting its crystallinity using laser irradiation.

While Wunderlich (1980) has discussed crystallization in detail, nucleation rate is a function of the free energy of nucleation barrier (ΔG), which is a function of undercooling ($\Delta T = T_m - T_c$, T_m: equilibrium melting temperature and T_c: crystallization temperature) and the free energy of activation (ΔG_η). Nucleation rate increases rapidly close to glass transition reaching a maximum at $T_c = T_c^*$ which is of the order of 105-110˚C in PLLA. During laser processing large deviations from T_m occur and hence the final development of crystallinity is expected not to be limited by the nucleation barrier but growth kinetics. According to the widely accepted *Lauritzen-Hoffman Theory (1976),* the growth Rate G of the crystal can be simplified as:

$$G = G_0 \exp\left(-\frac{U^*}{R(T_C - T_\infty)}\right)\exp\left(-\frac{K_g}{T_C \Delta T f}\right) \qquad (1)$$

where; K_g is the nucleation constant; $f = 2T/(T_m+T)$ is a factor accounting for heat of fusion change due to deviation from T_m , U^* is the activation energy of segment transport, R the gas constant, T_∞ the temperature at which no motion is seen and G_0 is the front factor (relatively independent of temperature). In case of PLLA, primarily regime II growth i.e. high nucleation rate with low growth velocity is seen during isothermal crystallization.

Laser processing requires a non-isothermal approach to overall crystallization as described by Nakamura, et al. (1972). The heat balance in

unit mass can be described by

$$\frac{d\phi(t)}{dt} = \frac{R(T - T_s)}{\Delta H} + \frac{C_p}{\Delta H}\frac{dT}{dt} \quad (2)$$

where Φ is the mass fraction of the transformed polymer, ΔH the heat of crystallization, R the heat transfer coefficient to surroundings at temperature T_s and C_p the mean specific heat of the polymer. The equation can be solved to obtain $T(\tau)$, the temperature during cooling and transformed fraction as a function of time can be simplified to Avrami form as:

$$\phi(t) = 1 - \exp\left[-\left(\int_0^t K(T(\tau))d\tau\right)^m\right] \quad (3)$$

where, $K(T) = k(T)^{1/m}$ and $k(T)$ is the isothermal crystallization rate constant, and depends on the shape of the growing crystallites and type and no. of nuclei formed, m is the Avrami Exponent which depends on nucleation type and growth geometry.

III. EXPERIMENTS

A. Sample Preparation

PLLA pellets with less that 0.01% residual solvent and less that 0.01% residual monomer were obtained from PURAC America. Films of average thickness 15-30 μm were prepared by solvent casting and similar thickness used for a batch of experiments. Pellets were dissolved in methylene chloride (0.1g/3ml, Sigma Aldrich), stirred for 3 hours, cast in a glass dish and left to settle for 10 hours at –20 ˚C. The film was cut into 15mm x 15mm squares, dried for 24 hrs prior to use and subsequently annealed at 110˚C for 3 hours. Amorphous samples were obtained by melting at 200 ˚C for 3 minutes and quenching in dry ice.

B. Experimental Set-up and Characterization

The experimental set-up (Fig. 1) consists of a Q-switched Nd: YAG laser operating at 355 nm in TEM00 mode with pulse duration of 50 ns and a repetition rate of 1 kHz. The laser beam diameter used was 28 μm, scan velocity optimized at 3mm/s and the fluence varied from 30-50 J/cm^2. The sample was placed in a holder on synchronized XYZ stages and a 9mm x 5mm area laser treated in air. 355 nm wavelength was selected for irradiation as the photon energy is below the bond breaking energy of C-C and C-H bonds allowing for primarily thermal effects which are beneficial to induce melting and structural changes as opposed to photochemical bond breakage that can occur at shorter wavelengths. The microstructure of the surface and microtomed sample cross-section was observed with the aid of a SEM (JEOL JSM-5600 LV) at voltages of 3-5 kV after gold coating (4-6 min). For cross-section observation, thicker 300 μm thickness samples were used for ease of microtoming.

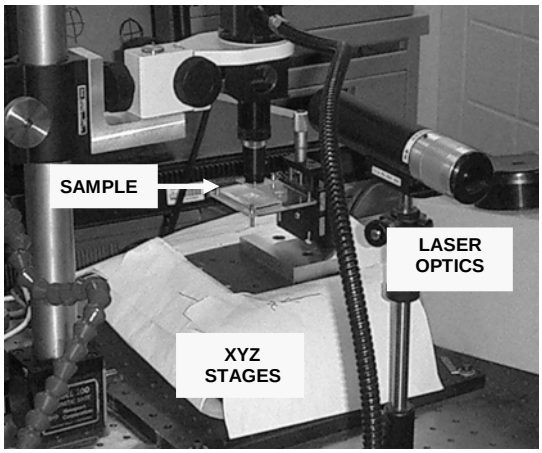

FIGURE 1. EXPERIMENTAL SET-UP.

WAXD measurements were carried out using an Inel X-ray diffractometer. Film specimens were exposed to monochromatic Cu Kα radiation (λ=1.542 Å) at 30 kV and 30 mA. Mass Absorption Coefficient calculated for PLLA indicates that X-rays penetrate through the bulk of the film. Thermo-Nicolet FTIR spectrophotometer with ATR (attenuated total reflectance) attachment using a ZnSe crystal (45˚) and 4 cm^{-1} resolution was used for measuring the IR spectrum of the samples (averaged over 128 scans) and analysed by Omnic software. Care was taken to ensure reproducible pressure between the sample and crystal for a set of experiments, each measurement repeated at least twice and ATR correction applied to normalize the effect of wavelength dependence. The depth of penetration was estimated to be 0.98-2.8 μm in the wave number range from 2000-650 cm^{-1}.

IV. RESULTS AND DISCUSSION

The surface morphology of the solution cast and annealed polylactide films observed under SEM is shown in Fig. 2. Spherulitic aggregations

that were partly merged were observed and confirmed with the optical microscope.

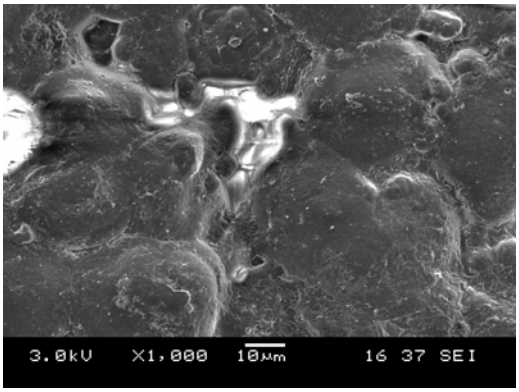

FIGURE 2. SURFACE MORPHOLOGY OF PLLA SAMPLE FILMS AS OBSERVED UNDER SEM.

A. Crystallinity Modification : WAXD

The crystal structure of PLLA has been well studied and three different crystal modifications are seen; viz the α, β, and γ-form depending on processing conditions. The α-form is the most commonly observed polymorph with an orthorhombic unit cell with 2 10_3 (3 monomeric units per 10 Å rise) polymeric helices. The unit cell dimensions indicated by Marega, et al. are a= 10.7 Å; b= 6.126 Å and c= 28.939 Å. The X-ray diffraction profile of untreated, treated (40J/cm^2), amorphous sample and background scatter are shown in Fig. 3. Crystallinity of the samples was determined based on simplifications of the *Ruland Method* as discussed by Alexander (1969). Background scattering was separated and amorphous fraction fit using a Gaussian profile. Mass fraction of the crystalline phase (crystallinity: Φ_c) was obtained by dividing the total intensity of the crystalline reflection with the total intensity. Disorder factor due to lattice defects and thermal disorder was not considered. The most prominent peak is seen at 16.7˚ representing the (110/ 200) reflections and smaller peaks at 14.7˚ and 19.1˚ representing the planes with miller indices of (010) and (203) respectively. This agrees with the α-form of PLLA consistent with other observations in literature for solution grown crystals.

Crystallite thickness can be measured using the *Scherrrer Equation* $t_{hkl} = k\lambda / B_{hkl} \cos\theta$ where, t_{hkl} is the crystallite size perpendicular to the plane (*hkl*), *K* the crystallite shape factor (0.9), λ the wavelength, B_{hkl} the width at half-maximum and θ the Bragg angle. The crystallite thickness was calculated to be in the range of 15-20 nm (110/200 reflection) as seen in Fig 11.

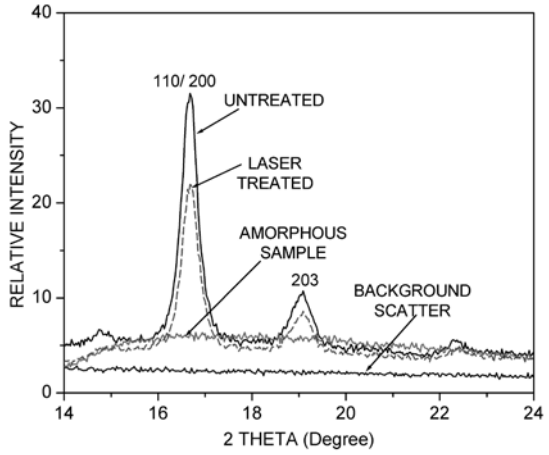

FIGURE 3. WAXD PROFILES OF UNTREATED, LASER TREATED (40 J/CM^2) AND AMORPHOUS SAMPLE AND BACKGROUND SCATTER. NOTE REDUCTION IN 110/200 AND 203 PEAKS.

The WAXD profiles of the crystalline fraction of untreated sample and irradiated at increasing fluences are shown in Fig. 4. There is a reduction in the intensity of both (110/200) and (203) peaks which indicates that the laser treatment primarily resulted in reduced order perpendicular to the helical chain direction and hence sample crystallinity.

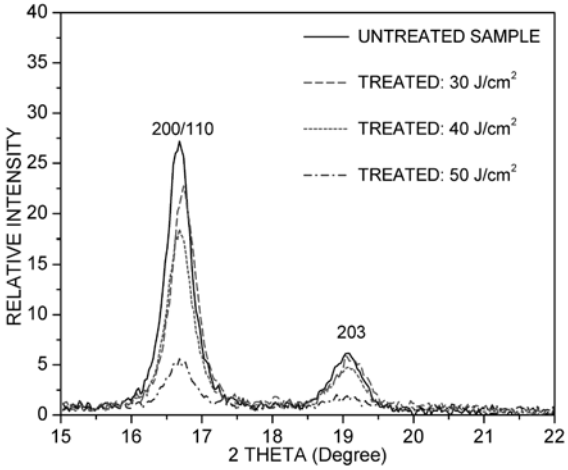

FIGURE 4. WAXD PROFILES INDICATING EFFECTS OF LASER FLUENCE ON THE CRYSTALLINE FRACTION OF PLLA SAMPLE.

Figure 11 indicates the effect of laser fluence on the measured mean crystallinity and crystallite thickness (bars indicate standard errors). The crystallinity of the sample was reduced by 7-8% for lower intensities to almost half at higher fluences. Since, WAXD provides integral intensity data from the complete depth

of the sample film, this can be attributed both to increased energy input causing melting of crystallites at progressively increasing depths in the sample films and more complete melting at higher temperatures in the surface regions.

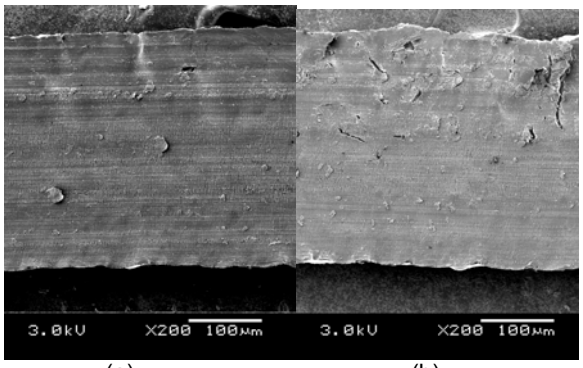

(a) (b)

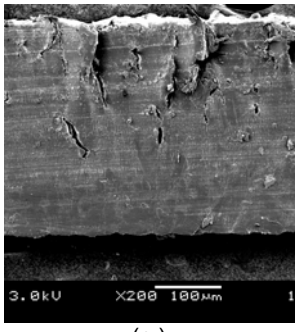

(c)

FIGURE 5. SEM IMAGES OF 300 µm (a) UNTREATED SAMPLE AND FILMS TREATED AT (b) 30 J/CM2 AND (c) 50 J/CM^2 INDICATING INCREASED CRAZING WITH FLUENCE.

While he crystallite thickness is not observed to change considerably, mean crystallite thickness reduces at higher fluences which indicates that disruption of structure might stem from partial melting at lower fluence regimes and more complete melting of high melting crystals at higher fluence, causing random displacement. This would explain why no significant broadening occurs in the XRD profiles and the main effect seen on irradiation is a reduction in the measured intensity. Figure 5. shows the SEM images of the untreated 300 µm sample and those treated at 30 and 50 J/cm^2 respectively. While no direct melting regions can be distinguished, it is apparent that there the affected depth increases with increased fluence. Crazing has been widely observed in semi-crystalline polymers and it has been suggested by Friedrich (1983) that crazes are initiated between the amorphous regions zones between the crystal lamella, which is in accordance with our observations.

B. Conformational Modification: ATR-FTIR

FTIR spectroscopy can provide information regarding chain conformations and crystallinity in semicrystalline polymers. ATR-FTIR spectrum of untreated, laser treated at 30 J/cm^2 and amorphous PLLA film are shown in Fig. 6.

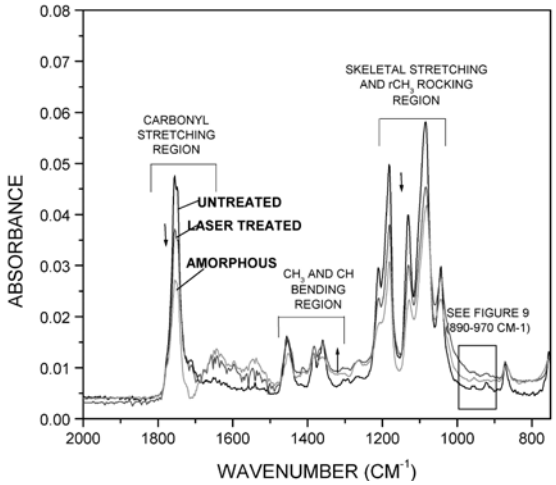

FIGURE 6. FTIR SPECTRA OF UNTREATED, TREATED (30J/CM^2) AND AMORPHOUS SPECIMENS (2000-700 CM^{-1}) INDICATING IMPORTANT BENDING, STRETCHING AND ROCKING MODES OF PLLA.

It can be seen that the Carbonyl (C=O) stretching region, CH_3 and CH bending region, and skeletal stretching (C-O-C) regions of original crystalline PLLA show sharper peaks with band splitting and a band at 920 cm^{-1} in accordance with observations from Kister, et al. The PLLA monomer **[-O-CH(-CH_3)-C(=O)-]$_n$** has three skeletal bonds C-O (ester), O-C_α and C_α-C; with the ester bond assumed to exist always in the *trans* conformation. From minimum energy calculations (Brant et al.), it is seen that four rotational isomeric states are feasible: *tt, tg,, gt* and *gg* corresponding to *trans* angles of -160˚, 160˚ and *gauche* angles of -73˚ and -48˚ respectively. The *gt* conformers have the lowest energy and correspond to a 10_3 helix. While the simulated spectrum shows 55% *gt*, 37% *gg* conformers and 4% each of other bent conformations; experimentally *gg* conformers (a 4_1 helix) are seen to be much lower and more *tt* conformers are seen which give extended chains but do not challenge the stiffness shown in PLLA chains.

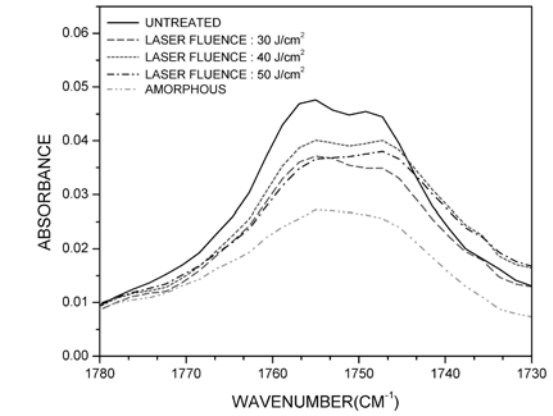

(a)

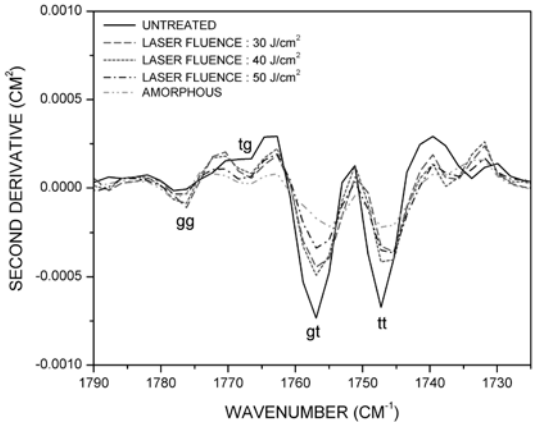

(b)

FIGURE 7. (a) C=O STRETCHING AND (b) DERIVATIVE SPECTRUM INDICATING THE PRIMARY CONFORMATIONS AND FACTOR GROUP SPLITTING WITH VARYING FLUENCE.

Following this analysis, Meaurio, et al. have observed that the carbonyl region of PLLA splits into four peaks during crystallization corresponding to different conformations due to intramolecular coupling. The details of the C=O stretching region (1790-1730 cm^{-1}) and the corresponding second derivatives are shown in Fig. 7. Pronounced splitting is seen in the original sample with broad peak in the amorphous sample and the treated samples show reduced spiltting with increasing fluence. Second derivative spectrum indicates peaks at 1776.2, 1766.7, 1757 and 1747 cm^{-1} corresponding to the gg, tg, gt and tt conformers with the latter two slightly shifted with respect to the transmission spectra peaks observed in literature. Fewer *gg* conformers are observed. The CH_3 and CH bending region in Fig. 6 (1250-1400 cm^{-1}) also indicates broadening with irradiation. The skeletal stretching region of PLLA (1050-1260 cm^{-1}) and its derivative spectrum are shown in Fig. 8, consisting of asymmetric C-O-C stretching vibrations. These modes split into 1180/1192 and 1210/1222 for the cold crystallized samples while no/reduced splitting is seen in the laser processed samples suggesting reduced crystal perfection.

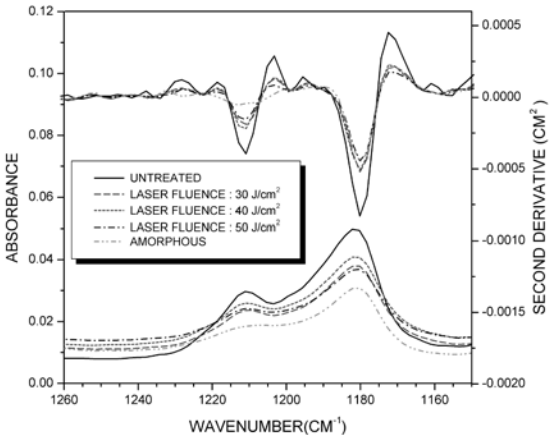

FIGURE 8. FTIR ABSORBANCE AND DERIVATIVE SPECTRUM OF THE SKELETAL STRETCHING REGION OF PLLA.

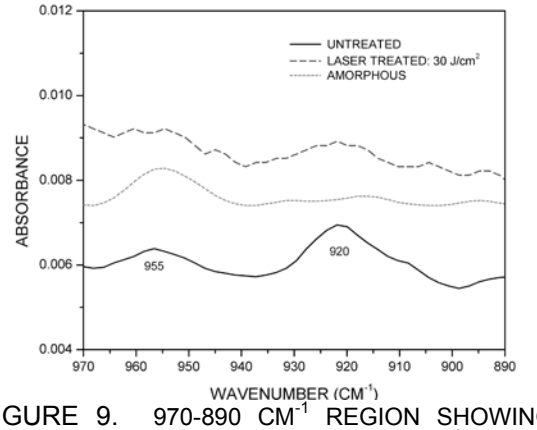

FIGURE 9. 970-890 CM^{-1} REGION SHOWING REDUCTION IN THE BAND AT 920 CM^{-1} AFTER PROCESSING (COUPLING OF THE vC-C STRETCH WITH CH_3 ROCKING MODE).

Fig. 9 (970-850 cm^{-1} region) shows that the band at 920 cm^{-1} reduces while peak at 955 cm^{-1} increases slightly upon laser processing with significant increase seen at higher fluences. The 920 cm^{-1} band was assigned to coupling of the vC-C backbone stretch with CH_3 rocking mode in 10_3 helical conformation of PLLA in line with Kister, et al. (1998).

XRD indicates a 10_3 helical structure (α-form) of PLLA and from IR spectra the *gt* conformers represent the crystalline conformers. Hence, *gt* peaks can be used to understand the effect of laser fluence. Spectral curve fitting was used in

Fig. 10 for untreated samples to obtain the heights of the peaks at 1757 cm^{-1} (*gt* conformers). Similarly, the effect of fluence is demonstrated by comparing the reduction in peak heights of *gt* conformers (Fig 11) which follows the same trend as WAXD. While this band represents added contributions from the *gt* conformers in the crystal lamellae and the interphase regions, the reduction has to be attributed to conformation changes happening in the crystal domains of the polymer.

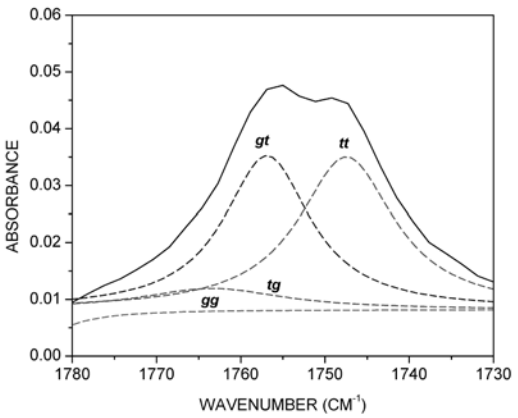

FIGURE 10. CURVE FITTING FOR CONFORMERS IN THE CARBONYL REGION (UNTREATED SAMPLE).

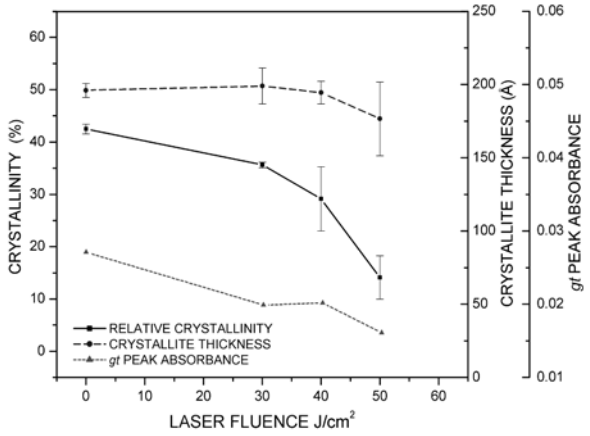

FIGURE 11. EFFECT OF LASER FLUENCE ON CRYSTALLINITY AND CRYSTALLITE THICKNESS OF PLLA (WAXD) AND *gt* PEAK ABSORBANCE FROM CURVE FITTING OF C=O REGION (FTIR SPECTRA).

The reduction is less drastic as compared with the WAXD peaks due to fixed penetration depth of ATR-IR spectrum. However, the reduction in conjunction with reduced lamellar thickness may imply transition from partial to complete melting at higher fluences in the layer at the surface probed by the ATR crystal.

C. Additional Comments

Due to rapid melting kinetics in polymers with low superheating, the surface of the material would experience melting temperatures and an increase in the affected depths would be expected with increase in fluence due to higher temperatures away from the surface which would explain the variation in crystallinity with fluence seen in WAXD and SEM. In addition, at critical temperatures close to and below the melting point conformational disorder can increase. This along with presence of low melting crystals might contribute to an increase in interlamellar material, leading to partial melting at depths higher than those seen by considering melting temperatures alone. As seen in Fig. 11, the reduction in intensity of the *gt* conformer peak is more pronounced at higher fluences and considering that the probed depth is fixed for FTIR (~2 μm) this may indicate that more complete melting is seen at higher fluences in the surface regions. Also, FTIR results do not indicate any new bands suggestive of degradation. At 355nm, the photon energy $E = 1245/\lambda = 3.5eV$ is not enough for direct bond breaking and hence photochemical effects would be expected to be negligible.

The cooling rates during the laser pulse are rapid and due considerable rapid undercooling during the pulse duration and considering dependence of nucleation on undercooling ΔT (section II), nucleation may be considered non-limiting and growth will primarily govern crystallinity evolution. Vasanthkumari and Pennings (1983) have shown that growth in PLLA follows regime II kinetics based on Kg values in equation (2). Maximum spherulite growth rates seen are around 130˚C (5μm/min). In this light, the overall development of crystallinity can be estimated. In literature, Avrami exponent for PLLA (*m)* is of the order of 3 and *k* values in the range of 5e-8 to 8e-10. From the laser quench rate *T(t)*, the values of *K(T(t))* in non-isothermal Avrami equation (4) can be obtained. In future, we expect to use obtain actual *T(t)* values using numerical methods. Considering, a single pulse at 1 msec (at 1 kHz) the value of the integral crystallization rate constant in equation (3) is expected to be small contributing to a small degree of transformation Φ so that the transformed material would be amorphous.

V. CONCLUSIONS

It has been shown that nanosecond laser irradiation at 355nm can be used to reduce the crystallinity of biodegradable polymer L-PLA and final crystallinity is a function of the fluence. WAXD results show increased reduction in intensities perpendicular to the helical PLLA axis with reduced overall crystallinity with increase in fluence. FTIR spectra exhibit broadening, smaller factor group splitting and reduction in *gt* conformers as fluence increases, which also confirms that these conformers primarily crystallize in the α-form. Rapid surface melting, high laser quench rates and primarily regime II kinetics of PLLA contribute to an overall reduction in crystallinity. Partial melting may be an important contributory factor. Laser surface treatment can potentially allow for an automated process that can spatially control the surface morphology and hence degradation associated with a different crystallinity at the surface.

ACKNOWLEDGEMENTS

Financial support from Columbia University and PURAC America's contribution with PLLA sample material is acknowledged. Prof. J. Koberstein's invaluable discussions are sincerely appreciated. Assistance from Prof. Helen Lu's group for sample preparation and Dr. Louis Avila for FTIR equipment is also highly appreciated. This work used equipment at the Columbia University MRSEC supported by NSF DMR-0213574.

REFERENCES

Aguilar, C.A., Y. Lu, S. Mao, and S. Chen (2005). "Direct Micro-Patterning of Biodegradable Polymers Using Ultraviolet and Femtosecond Lasers," Biomaterials, 26(36), pp. 7642-7649.

Alexander, L. (1969). X-Ray Diffraction Methods in Polymer Science, Wiley-Interscience, NY.

Brant, D.A., A.E. Tonelli and P.J. Flory (1969). "The Configurational Statistics of Random Poly(lactic acid) Chains," Macromolecules, 2 (3), 228-235.

Dunn, D.S., and A.J. Ouderkirk (1990). "Chemical and Physical Properties of Laser-Modified Polymers," Macromolecules, 23(3), pp. 770-774.

Garlotta, D. (2001). "A Literature Review of Poly (Lactic Acid)," Journal of Polymers and the Environment, 9(2), pp. 63-84.

Friedrich, K. (1983) "Crazes and Shear Bands in Semi-Crystalline Thermoplastics," Advances in Polymer Science, 52/53, Springer-Verlag.

Hoffman, J.D., G.T. Davies, and J.I. Lauritzen (1976). Treatise on Solid-State Chemistry Vol. 3, Chapter 15, Plenum Press, New York.

Kister, G., G. Cassanas, and M. Vert (1998). "Effects of Morphology, Conformation And Configuration on the IR and Raman Spectra of Various Poly (Lactic Acid) s," Polymer, 39 (2), pp. 267-273.

Lazare, S., and P. Benet (1993). "Surface Amorphization of Mylar Films with Excimer Laser Radiation Above and Below Ablation Threshold," Journal of Applied Physics, 74(8), pp. 4953-4957.

Marega, C., A. Marigo, V. Di Noto, and R. Zannetti, (1992) "Structure and Crystallization Kinetics of Poly (L-Lactic Acid)," Makromol. Chem., 193 (7), pp. 1599-1606.

Meaurio, E., N. Lopez-Rodrıguez, and J.R. Sarasua (2006), "Infrared Spectrum of Poly(L-lactide): Application to Crystallinity Studies," Macromolecules, 39 (26), pp. 9291-9301.

Nakamura, K., T. Watanabe, K. Katayama, and T. Amano (1972). "Some Aspects of Nonisothermal Crystallization of Polymers. I.," Journal of Applied Polymer Science, 16(5), pp. 1077-1091.

Tsuji, H., and Y. Ikada (1998). "Properties and Morphology of Poly (L-Lactide) II," Journal of Polymer Sci., Part A: Polymer Chem., 36 (1), pp. 59-66.

Vasanthakumari, R., and A.J. Pennings (1983). "Crystallization Kinetics of Poly(L-Lactic Acid)," Polymer, 24(2), pp. 175-178.

Wunderlich, B. (1976). Macromolecular Physics, Vol. 2, and (1980), Vol. 3, Academic Press, NY.